

Massive-Star Mergers and the Recent Transient in NGC4490: A More Massive Cousin of V838 Mon and V1309 Sco

Nathan Smith^{1*}, Jennifer E. Andrews¹, Schuyler D. Van Dyk², Jon C. Mauerhan³, Mansi M. Kasliwal⁴, Howard E. Bond^{5,6}, Alexei V. Filippenko³, Kelsey I. Clubb³, Melissa L. Graham², Daniel A. Perley^{4,7}, Jacob Jencson^{4,8}, John Bally⁹, Leonardo Ubeda⁶, Elena Sabbi⁶

¹Steward Observatory, University of Arizona, 933 N. Cherry Ave., Tucson, AZ 85721, USA

²Spitzer Science Center/Caltech, Mail Code 220-6, Pasadena, CA 91125, USA

³Department of Astronomy, University of California, Berkeley, CA 94720-3411, USA

⁴Astronomy Department, California Institute of Technology, 1200 E. California Boulevard, Pasadena, CA 91125, USA

⁵Department of Astronomy & Astrophysics, Pennsylvania State University, University Park, PA 16802, USA

⁶Space Telescope Science Institute, 3700 San Martin Dr., Baltimore, MD 21218, USA

⁷Dark Cosmology Centre, Niels Bohr Institute, University of Copenhagen, Denmark

⁸NSF Graduate Fellow

⁹Center for Astrophysics and Space Astronomy, University of Colorado, 389 UCB, Boulder, CO 80309, USA

2 August 2021

ABSTRACT

The Galactic transient V1309 Sco was the result of a merger in a low-mass star system, while V838 Mon was thought to be a similar merger event from a more massive B-type progenitor. In this paper we study a recent optical and infrared (IR) transient discovered in the nearby galaxy NGC 4490 named NGC 4490-OT2011 (NGC 4490-OT hereafter), which appeared similar to these merger events (unobscured progenitor, irregular multi-peaked light curve, increasingly red colour, similar optical spectrum, IR excess at late times), but which had a higher peak luminosity and longer duration in outburst. NGC 4490-OT has less in common with the class of SN 2008S-like transients. A progenitor detected in pre-eruption *Hubble Space Telescope* (*HST*) images, combined with upper limits in the IR, requires a luminous and blue progenitor that has faded in late-time *HST* images. The same source was detected by *Spitzer* and ground-based data as a luminous IR (2–5 μm) transient, indicating a transition to a self-obscured state qualitatively similar to the evolution seen in other stellar mergers and in luminous blue variables. The post-outburst dust-obscured source is too luminous and too warm at late times to be explained with an IR echo, suggesting that the object survived the event. The luminosity of the enshrouded IR source is similar to that of the progenitor. Compared to proposed merger events, the more massive progenitor of NGC 4490-OT seems to extend a correlation between stellar mass and peak luminosity, and may suggest that both of these correlate with duration. We show that spectra of NGC 4490-OT and V838 Mon also resemble light-echo spectra of η Car, prompting us to speculate that η Car may be an extreme extension of this phenomenon.

Key words: binaries: general — circumstellar matter — stars: evolution — stars: massive — stars: winds, outflows

1 INTRODUCTION

Ongoing dedicated studies of the transient sky are revealing an increasingly wide diversity of explosive and eruptive stellar transients that are less luminous than traditional super-

* E-mail: nathans@as.arizona.edu

novae (SNe), but more luminous than classical novae. There is a broad range of theoretical mechanisms that might account for these, yet linking physical mechanisms to individual observed phenomena remains challenging. Extragalactic events being discovered in modern transient surveys occur at distances where detailed information about the progenitor star or potential surviving star is scarce, complicating any connection to observed Galactic populations.

More than a decade ago, few such events were known, and the transients with luminosities between those of novae and SNe were generally linked to the class of eruptive massive stars known as luminous blue variables (LBVs; Humphreys & Davidson 1994). Names like SN impostors, Type V SNe, or η Carinae variables were often taken to be synonyms of LBVs (Humphreys & Davidson 1994; Humphreys, Davidson, & Smith 1999; Van Dyk et al. 2000). With the increasing observed diversity of the SN impostor-like transients, however, some differentiation in observed properties also developed. Proposed observational subclasses include LBV giant eruptions (Smith et al. 2011), SN 2008S-like events (Thompson et al. 2009; Prieto et al. 2008; Kochanek 2011), and a class of luminous red variables that have been linked to collisions and merger events (see below).

The SN 2008S-like sources, including the well-studied event NGC 300-OT2008 (Bond et al. 2009) and its kin, seem to be distinguished in that they have heavily dust-enshrouded progenitors, more monotonic optical light-curve evolution, strong [Ca II] and Ca II emission features, and strong infrared (IR) excess at late times (Thompson et al. 2009; Prieto et al. 2008; Kochanek 2011). Some LBVs share these properties (Smith et al. 2011), but the SN 2008S-like progenitors tend to have lower luminosities and implied masses (Thompson et al. 2009; Prieto et al. 2008; Kochanek 2011) than the recognized mass and luminosity ranges for LBVs (Smith, Vink, & de Koter 2004a). In addition, unlike LBVs, there is no clear sign that SN 2008S-like transients survive the event (Adams et al. 2015). The class of red transients identified as possible mergers also tend to have lower-mass progenitors when this information is available, but their progenitors do not appear to be as heavily enshrouded in dust as the SN 2008S-like objects. Moreover, the SN 2008S-like objects and the lower-mass merger outbursts seem to trace different Galactic stellar populations. In this paper, we suggest a new potential member of this class of merger objects, but with a higher initial mass than any object in this class studied so far. This new object in NGC 4490 also shares many properties in common with giant LBV eruptions, so the distinction between LBVs and merger events may be blurry.

Tylenda et al. (2011) presented the most direct and dramatic evidence linking one of these transients to a violent stellar merger event. They analyzed archival Optical Gravitational Lensing Experiment (OGLE) photometry and found that the progenitor of the 2008 Galactic transient V1309 Sco had been an eclipsing binary, and that the orbital period decreased rapidly leading up to the catastrophic transient event. The progenitor star was thought to have an initial mass of 1–2 M_{\odot} , while the transient event had a peak absolute magnitude of roughly -6.9 mag (V band; Vega-based magnitudes), although the distance is uncertain, and a duration of about a month. A brighter Galac-

tic event was the 2002 transient V838 Mon, with a peak absolute visual magnitude of about -9.8 , a longer duration of about 80–90 d, and a very irregular, multi-peaked light curve (Afşar & Bond 2007; Bond et al. 2003; Sparks et al. 2008). The progenitor of this transient was thought to be more massive (5–10 M_{\odot}), due to a small host cluster with B-type stars still on the main sequence (Rosero-Rueda et al. 2008; Afşar & Bond 2007). It also had a B3 V companion star that was engulfed by the expanding dusty ejecta several years after the outburst. V838 Mon is perhaps best known for the series of spectacular colour light-echo images taken by the *Hubble Space Telescope* (*HST*) (Bond et al. 2003).

Both V1309 Sco and V838 Mon started out with relatively smooth continuum emission plus narrow Balmer emission lines, but developed very red optical colours, atomic and molecular absorption features, and strong signatures of dust in their spectra as they faded (Munari et al. 2007; Mason et al. 2010; Nichols et al. 2013; Loebman et al. 2015). The observed properties of these transients appear to be consistent with theoretical expectations for merger events (Ivanova et al. 2013; Soker & Tylenda 2006, 2007). Other events that may belong to the same class are the Galactic transients V4332 Sgr in 1994 (Martini et al. 1999) and OGLE 2002-BLG-360 (Tylenda et al. 2013), and potentially also the historical Galactic novae CK Vul (Kato 2003; Kaminski & Menten 2015), and V1148 Sgr (Mayall 1949). Proposed extragalactic counterparts include M31 RV (Rich et al. 1989; Bond & Siegel 2006; Bond 2011), M85 OT2006-1 (Kulkarni et al. 2007), and the transient in M31 discovered in January 2015 (Kurtenkov et al. 2015; Williams et al. 2015). Kochanek et al. (2014) have estimated the Galactic rates for merger events and found them to be quite common, with approximate values of 0.1 yr^{-1} for fainter events like V1309 Sco, and 0.03 yr^{-1} for brighter events like V838 Mon. Kochanek et al. (2014) also suggest that the peak luminosity of the resulting transient is a steep function of the stellar mass, similar to the mass-luminosity relation on the main sequence.

In this paper we discuss the bright optical and IR transient source that appeared in 2011 in the host galaxy NGC 4490, and we demonstrate that it bears some interesting similarities to the class of mergers discussed above. We also point out that despite its similar peak luminosity, this new event appears to have less in common with SN 2008S-like transients. The object was first recognized as a transient in the optical, so for brevity we refer to it here as NGC 4490-OT, although subsequently it was also shown to be a transient source in the thermal IR. It is also designated as PSN J12304185+4137498, and in our IR transient search described below it was found independently and named SPIRITS 14pz.

NGC 4490-OT was discovered in unfiltered CCD images on 2011 Aug 16.83 (UT dates are used throughout this paper) by Cortini & Antonelli (2011), located $57''$ west and $37''$ south of the bright centre of the nearby galaxy NGC 4490. Its coordinates are $\alpha_{2000} = 12^{\text{h}}30^{\text{m}}41^{\text{s}}.84$; $\delta_{2000} = +41^{\circ}37'49''.7$. NGC 4490 is part of a pair of actively star-forming interacting galaxies (the other galaxy in the pair is NGC 4485; see Figure 1), and NGC 4490 was also the host galaxy as for the Type IIb event SN 2008ax. Accord-

ing to the NASA Extragalactic Database (NED)¹, the host has an average redshift of $z = 0.00185$ (565 km s^{-1}). This would imply a distance of $d = 9.22 \text{ Mpc}$ and a distance modulus of $m - M = 29.82 \text{ mag}$. However, in their study of SN 2008ax, Pastorello et al. (2008) noted some inconsistencies in the distances to the two galaxies in the interacting pair and derived an average distance combining several techniques of $d = 9.6 \text{ Mpc}$ and $m - M = 29.92 \text{ mag}$. We adopt these latter values here. We also adopt a line-of-sight Milky Way reddening of $E(B - V) = 0.019 \text{ mag}$ ($A_V = 0.06 \text{ mag}$, $A_R = 0.047 \text{ mag}$) from Schlafly & Finkbeiner (2011). There may be additional host-galaxy reddening (Pastorello et al. 2008 estimate $E(B - V) = 0.3 \text{ mag}$ for SN 2008ax, which is in a similar part of the galaxy), or circumstellar reddening, but we consider these in more detail later.

With the above adopted parameters, the discovery brightness of the transient corresponds to an absolute magnitude (assumed to be roughly R band) of about -13.3 mag . As discussed below, the peak luminosity 100–200 d later is somewhat higher, around -14.2 mag (with the additional host-galaxy reddening that we favor in the discussion below, the peak would be about -15 mag). This implies that the object may be related to the broad class of SN impostors that are less luminous than core-collapse SNe. Early classification spectra obtained on 2011 Aug. 18.9 and 19.9 (days 2–3 after discovery) showed a blue continuum and bright, narrow Balmer emission lines, plus some fainter Fe II lines (Magill et al. 2011), qualitatively similar to known spectra of LBV eruptions (Smith et al. 2011). However, Magill et al. (2011) noted that there was no bright, blue star known at that position in previously obtained archival *HST* images, while archival *Spitzer* data did not reveal a bright mid-IR source either, apparently disfavouring a very luminous LBV progenitor.

Fraser et al. (2011) conducted a more detailed analysis of the archival *HST* images, and proposed that a source at the nominal position of the transient was a likely progenitor detection, with an absolute magnitude -6.2 in the F606W filter in the mid 1990s. (With the somewhat different distance and reddening we adopt, this corresponds to -6.4 mag .) This is much brighter at visual wavelengths than the heavily dust-enshrouded progenitors of SN 2008S and NGC 300-OT (Prieto 2008; Prieto et al. 2008; Thompson et al. 2009), and only modestly fainter than the -7.5 mag progenitor of the LBV-like transient UGC 2773-OT (Smith et al. 2010a, 2016) and the LBV progenitor of the SN 1954J eruption (Tammann & Sandage 1968; Smith et al. 2001; Van Dyk et al. 2005). This may suggest that the progenitor and its outburst are related to the LBV phenomenon in more massive stars, but as we detail below, it also shares some interesting properties with lower-luminosity transients that are thought to arise from stellar merger events.

Table 1. *HST* Imaging and photometry of NGC 4490-OT

Date	Instr	Day	Filter	mag ^a	σ
1994 Dec 03	WFPC2	−6100	F606W	23.58	0.24
2013 Oct 30	WFC3-UVIS	805	F275W	23.68	0.07
2013 Oct 30	WFC3-UVIS	805	F336W	25.36	0.23
2013 Oct 30	WFC3-UVIS	805	F438W	25.43	0.10
2013 Oct 30	WFC3-UVIS	805	F555W	25.33	0.05
2013 Oct 30	WFC3-UVIS	805	F814W	23.40	0.04

^a The 1994 magnitude was measured in a $0''.5$ diameter aperture. The 2013 measurements are the result of PSF-fitting photometry from the LEGUS photometry catalog (see text). We also performed aperture photometry in a small $0''.5$ diameter aperture that yielded slightly different magnitudes, as discussed later.

Table 2. KAIT Unfiltered Photometry of NGC 4490-OT

Date	MJD	m^a	$m - 1\sigma$	$m + 1\sigma$
...	...	(mag)	(mag)	(mag)
2012 Jan 10	55936.55	15.793	15.776	15.810
2012 Jan 12	55938.40	15.794	15.778	15.811
2012 Jan 13	55939.54	15.799	15.782	15.816
2012 Jan 18	55944.48	15.779	15.763	15.795
2012 Jan 18	55944.48	15.795	15.781	15.809
2012 Jan 30	55956.42	15.954	15.933	15.974
2012 Feb 03	55960.44	16.035	16.016	16.053
2012 Feb 10	55967.47	16.419	16.399	16.439
2012 Feb 24	55981.29	17.430	17.375	17.486
2012 Mar 07	55993.35	17.988	17.868	18.109
2012 Mar 09	55995.39	18.336	18.173	18.500
2012 Mar 22	56008.34	18.887	18.739	19.038
2012 Apr 02	56019.42	(19.20)
2012 Apr 07	56024.42	(18.56)
2012 Apr 23	56040.37	(19.47)

^aUpper limits are indicated in parentheses.

2 OBSERVATIONS

2.1 Hubble Images

A portion of NGC 4490 including the position of the transient was observed by *HST* using the Wide Field Planetary Camera 2 (WFPC2) on 1994 Dec. 3 as part of program SNAP-5446 (PI G. Illingworth). The data consisted of a pair of CR-split 80 s exposures in the F606W filter. The location of the transient fell on one of the larger WF chips with $0''.1$ pixels. We obtained these pipeline drizzled images from the *HST* archive. This is the same image set that Fraser et al. (2011) used to identify a probable source as the progenitor of NGC 4490-OT. For this source identified by them we measure $m(\text{F606W}) = 23.58 \pm 0.24 \text{ mag}$ (1σ) using $0''.5$ diameter aperture photometry (Vega-based magnitudes). This agrees within the uncertainty with the magnitude reported by Fraser et al. (2011). With our adopted distance and extinction, it corresponds to an absolute magnitude for the progenitor of about -6.4 mag , roughly 6100 days prior to discovery of the optical transient outburst. The *HST*/WFPC2 grey-scale image of the progenitor is shown in the upper-left panel of Figure 1.

Here we confirm that this candidate was indeed the progenitor star of the NGC 4490-OT transient, since later *HST* images show that the same source has faded significantly after the outburst. The same position was imaged again with *HST* on 2013 Oct. 30, but this time with the WFC3-UVIS camera and using several broadband filters (see Table 1).

¹ <https://ned.ipac.caltech.edu/>

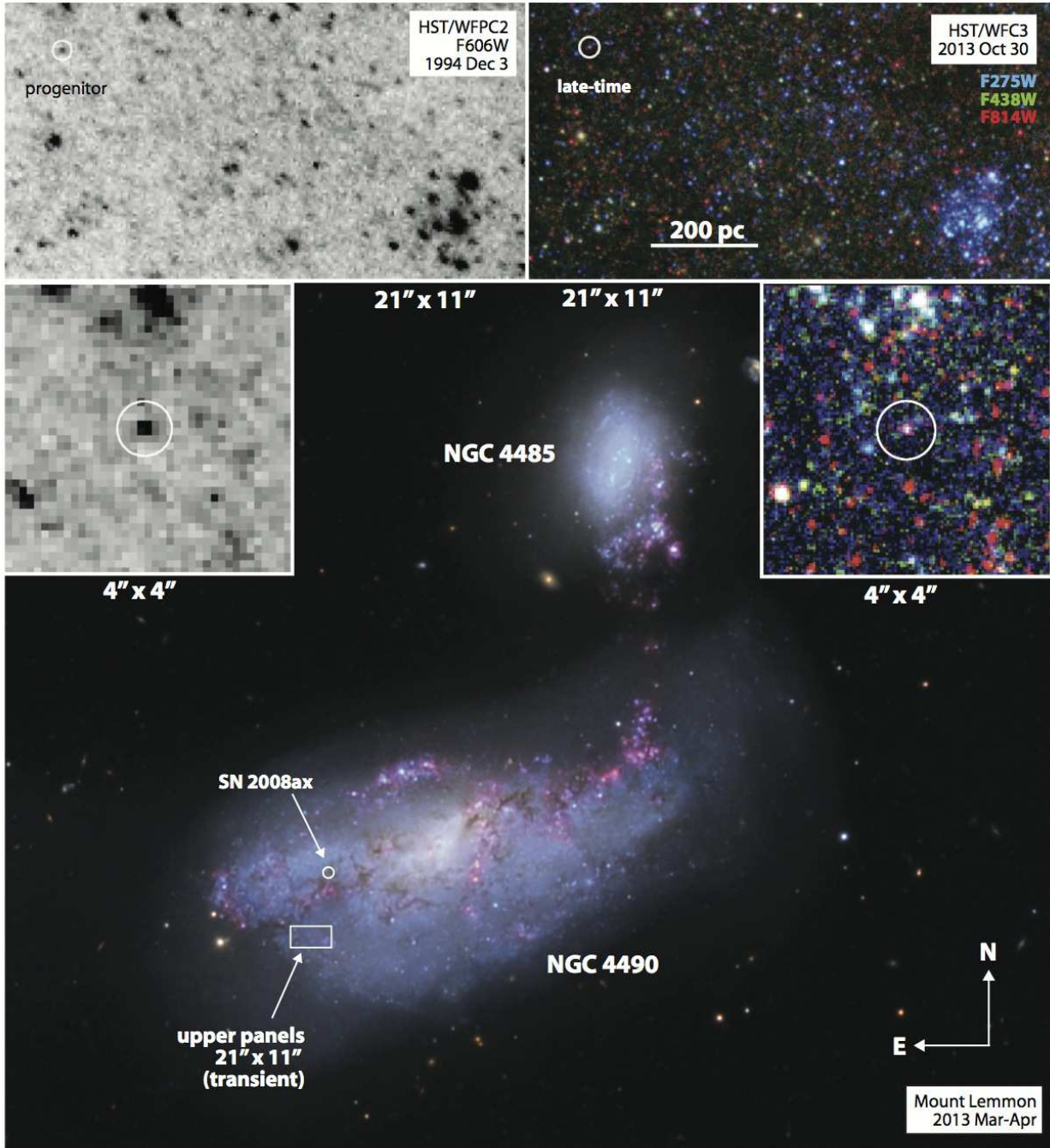


Figure 1. Images of the host environment of the NGC 4490 transient. The main image at the bottom shows a wide-field view of the interacting pair of galaxies NGC 4490 and NGC 4485. This colour image is a composite of individual visible-wavelength images taken on different nights during March and April 2013 using the 0.8 m Schulman Telescope at the Mount Lemmon SkyCenter (image credit: Adam Block/Mount Lemmon SkyCenter/University of Arizona; used with permission). This image is included to show the location and surrounding environment of the transient within the host galaxy. The small white rectangle in the lower left marks the immediate environment of the transient, corresponding to the $21'' \times 11''$ inset images at the top of the figure. The position of SN 2008ax is also noted. These insets show *HST* images, with the grey-scale image at left corresponding to the pre-eruption archival image taken with WFC2 in the F606W filter in 1994. The inset at right is a colour image made from F275W, F438W, and F814W frames obtained with the WFC3-UVIS camera after the eruption had faded in October 2013. In these images, the white circle marks the position of the NGC 4490-OT transient. The $4'' \times 4''$ boxes are zoomed-in sections of these same two *HST* frames.

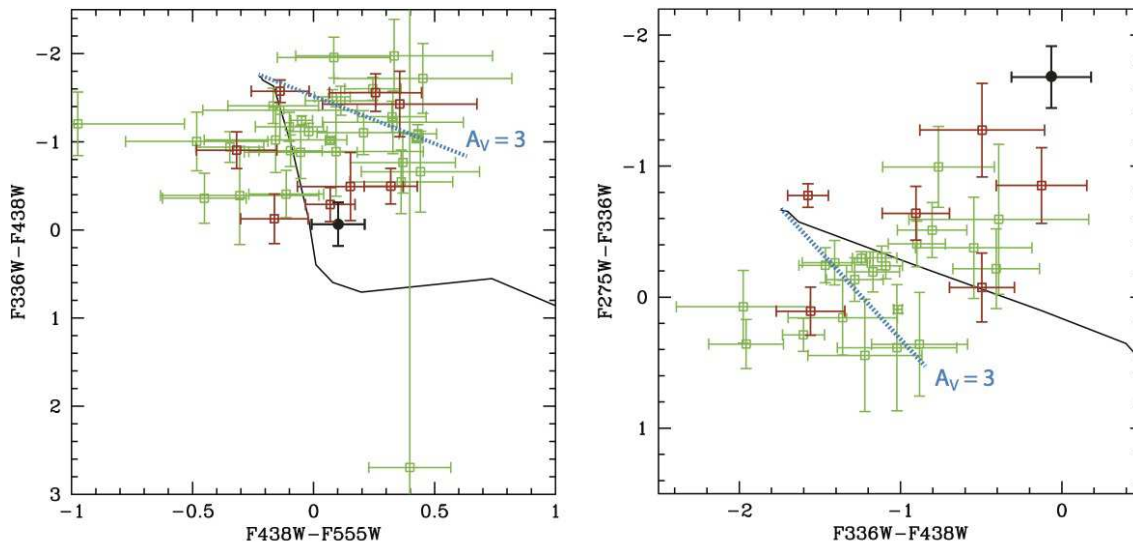


Figure 2. Colour-colour plots from *HST* LEGUS data taken at late times, produced as described in the text, Section 2.1. Green open squares correspond to detected sources within a projected separation of 100 pc from NGC 4490-OT, while red open squares are projected within 50 pc. The filled black circle is NGC 4490-OT at late times. The colour-colour locus for normal supergiants is shown by the black curve in both plots, and a reddening vector for $A_V = 3$ mag and $R = 3.1$ is shown by the blue dashed line.

These images were obtained as part of the Legacy Extra-Galactic UV Survey (LEGUS) project (PI Calzetti; GO-13364). The filters and corresponding Vega-based magnitudes of the same source are given in Table 1. Although these images do not have the same F606W filter as the progenitor images, both the F555W and F814W fluxes are fainter than the progenitor. A colour composite made from the F275W, F438W, and F814W images in 2013 Oct. is shown in the upper-right panels of Figure 1.

We also investigate the host environment around the transient. Photometry for sources in the environment of the OT was obtained from the Level-0 source list generated by the LEGUS project (see Calzetti et al. 2015). The individual LEGUS WFC3/UVIS ‘flt’ frames were first corrected for charge-transfer efficiency (CTE) losses using the available online tools². The corrected frames in each of the five LEGUS bands were then processed with Dolphot (Dolphin 2000), assuming a signal-to-noise ratio threshold of 3 (and with CTE correction turned off). No further selection criteria or cuts were imposed upon the data. The five-band source lists were then bandmerged, with the OBJECT-TYPE flag set to either ‘1’ or ‘2’ (i.e., a good star or one too faint for point-spread function determination) and the ERROR-FLAG < 1. We used the Level-0 lists, rather than the Level-1 list, which have further cuts imposed upon the photometry, in order to find as many sources in the OT environment as possible. However, the Level-0 list almost certainly contains a number of spurious sources. Following, for example, Gogarten et al. (2009), we considered star-like sources within a ~ 100 pc radius of the OT, since stars formed in a common event will remain spatially correlated up to this spatial scale for ~ 100 Myr. Gogarten et al. further limited the scale to ~ 50 pc around a source of interest as a compromise between including as many coeval stars as possible,

while limiting the amount of source contamination. We also consider this smaller spatial scale in our analysis below.

Figure 2 compares colours from the photometry, particularly in the ultraviolet (UV) and blue bands, to the colour-colour loci for normal supergiant stars, and also assumes a reddening vector following Cardelli, Clayton, & Mathis (1989) with $R_V = 3.1$. In Figure 2, sources within a 100 pc projected radius of NGC 4490-OT are green open squares, and those projected within 50 pc are red open squares. NGC 4490-OT itself is the filled black circle, although its UV colours (especially including F275W) may be peculiar owing to line emission. The implications for the local extinction toward NGC 4490-OT are discussed below in Section 3.1.

2.2 Optical Photometry

The early-time light curve of NGC 4490-OT after discovery is poorly sampled, because the object became difficult to observe owing to hour-angle constraints a few weeks after discovery. In Figure 3 we collect early unfiltered CCD magnitudes reported by amateur observers.³ Since these are not all on the same photometric system, we adopt representative error bars of ± 0.4 mag for the purpose of characterizing the early photometric behaviour. We emphasize, however, that these are not our measurements and we do not have adequate information to assess their true uncertainty; we only show them for comparison. Measurements by several different amateur observers agree that the source faded by ~ 1.5 mag in the first few weeks.

Our photometric monitoring of NGC 4490-OT commenced when the object returned from behind the Sun in January 2012. We used the Katzman Automatic Imaging Telescope (KAIT; Filippenko et al. 2001; Filippenko 2003)

² http://www.stsci.edu/hst/wfc3/tools/cte_tools.

³ See <http://www.rochesterastronomy.org/supernova.html>

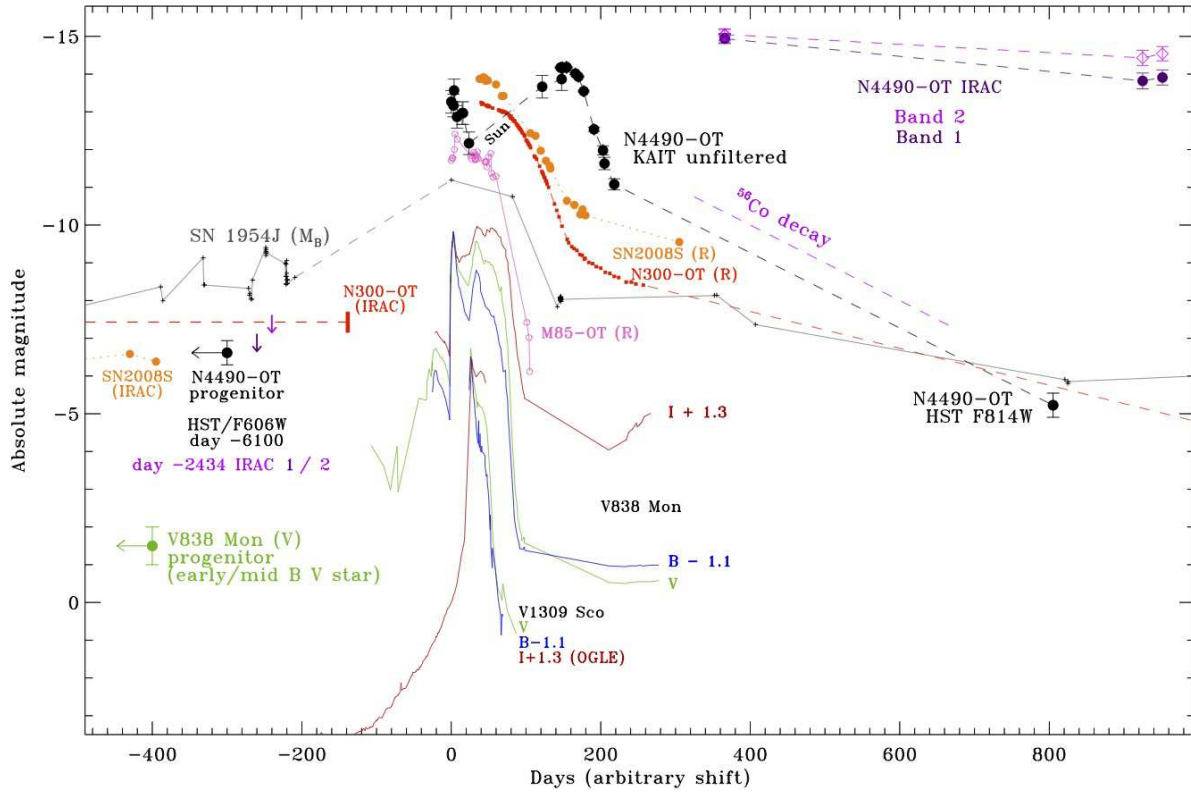


Figure 3. Photometry of NGC 4490-OT and some related transients. For NGC 4490-OT, we adopt the reddening and distance described in the text to place it on an absolute-magnitude scale for comparison with the other objects from the literature. The black dots correspond to NGC 4490-OT, which includes unfiltered (approximately R -band) photometry taken from initial reports for the first few weeks plus KAIT unfiltered photometry after it reappeared from behind the Sun. The earliest point represents the progenitor that we measured in archival *HST* F606W images taken approximately 6100 days prior to discovery, as well as a late-time measurement with *HST* in the F814W filter. See Table 1. Photometry for the other objects is taken from the literature as follows: SN 2008S R band (Smith et al. 2009) and IRAC, NGC 300-OT R band (Bond et al. 2009) and IRAC (Prieto 2008; Thompson et al. 2009), SN 1954J B band (Tammann & Sandage 1968), V838 Mon BVI bands (Bond et al. 2003; Sparks et al. 2008), the likely V838 Mon progenitor assumed to be an early/mid B star for reasons noted in the text (Rosero-Rueda et al. 2008; Afşar & Bond 2007), and the V1309 Sco I band from OGLE (Tylenda et al. 2011) and the V and B bands from AAVSO (the American Association of Variable Star Observers; see www.aavso.org). The R -band light curve of M85-OT is shown in pink for comparison, from Kulkarni et al. (2007).

Table 3. Spitzer Photometry of NGC 4490-OT

Date	MJD	IRAC1	1σ	IRAC2	1σ
...	...	(mag)	(mag)	(mag)	(mag)
2004 Dec 17	53356.04	(22.8)	...	(22.3)	...
2012 Aug 17	56156.03	14.97	0.12	14.89	0.15
2012 Aug 17	56156.18	14.98	0.13	14.87	0.15
2014 Feb 27	56715.32	16.10	0.21	15.49	0.20
2014 Mar 25	56741.84	16.01	0.20	15.38	0.19

Upper limits are indicated in parentheses.

at Lick Observatory to obtain unfiltered photometry. As demonstrated by Li et al. (2002), the best match to broad-band filters for the KAIT unfiltered data is the R band. We list the KAIT apparent unfiltered (approximately R) magnitudes of NGC 4490-OT in Table 2. To put the flux on an absolute-magnitude scale, we adopt the distance and reddening listed in the Introduction; the resulting absolute-magnitude light curve is shown in Figure 3, along with other transient sources from the literature for comparison.

2.3 IR Imaging

We observed the host galaxy NGC 4490 in the IR as part of the large program called SPitzer InfraRed Intensive Transients Survey (SPIRITS; PI M. Kasliwal), conducted using the Infrared Array Camera (IRAC; Fazio et al. 2004) Bands 1 and 2 (3.6 and 4.5 μm , respectively) during the *Spitzer* Space Telescope (*Spitzer*) warm mission in Cycle 10. Our observations were obtained on 2014 Feb. 27 and Mar. 25. A source coincident with the NGC 4490 optical transient was identified in the IR by comparison with archival *Spitzer* images obtained in the same filters in 2004 and 2012. No source was detected in the first epoch in 2004, so we used this set of images as a template to subtract from the 2012 and 2014 images. The resulting Band 1 and 2 magnitudes for various dates measured on template-subtracted images are given in Table 3. For the nondetection on the first epoch in 2004, we list upper limits in Table 3. These are 5σ upper limits based on the background noise measured in an annulus around the position of the source in the template images and the detection images added in quadrature. Experiment-

Table 4. Spectroscopic Observations of NGC 4490-OT

Date	Tel./Instr	Day ^a	$\Delta\lambda(\text{\AA})$	note	$T_{\text{BB}}(\text{K})$
2012 Jan. 18	Lick/Kast	154	3500–10,000	...	5100
2012 Jan. 19	MMT/BC	155	5700–7000
2012 Jan. 29	MMT/BC	165	3800–9000	clouds	...
2012 Feb. 01	Lick/Kast	168	3500–10,000	...	4700
2012 Mar. 01	MMT/BC	197	5700–7000	clouds	...

^aDay refers to approximate days after discovery, 2011 Aug 16.83.

ing with annuli that had a variety of inner and outer radii gave consistent results within ± 0.1 mag.

These IR magnitudes from detections in template-subtracted images, as well as 2004 progenitor upper limits, are plotted in Figure 3. The date of the progenitor upper limits from *Spitzer* corresponds to day -2434 , which is far off the left side of the plot in Figure 3, so the limits are shown shortly before the transient’s discovery for reference. For the IR absolute magnitudes, we assumed the same distance modulus of $m - M = 29.92$ mag as adopted above for optical data. The upper limits to the progenitor’s IR luminosity are comparable to the luminosity of the progenitor source detected in *HST* images. Thus, although we did not detect the IR flux of the progenitor itself, we can see that it is clearly not a heavily obscured progenitor dominated by IR emission as in the cases of SN 2008S and the 2008 transient in NGC 300. The optical-to-IR spectral energy distributions (SEDs) of the progenitor and late-time source are discussed later.

We also obtained a K_s -band image of the site of NGC 4490-OT on 2014 May 10, using WIRC on the Palomar 5-m telescope. This corresponds to day 997 after discovery, and is similar in time to our last epoch of *Spitzer* Band 1 and 2 photometry. The image was calibrated using 2MASS stars in the field, and we derive a K -band brightness of 18.7 ± 0.2 mag.

2.4 Optical Spectroscopy

We obtained five epochs of visible-wavelength spectroscopy during the sharp decline after the second luminosity spike that occurred around day 150; this also coincided with the time when NGC 4490 returned from behind the Sun and when our KAIT photometric monitoring began. We used the Bluechannel (BC) spectrograph on the 6.5-m Multiple Mirror Telescope (MMT) and the Kast spectrograph (Miller & Stone 1993) on the Lick 3-m Shane reflector, with observation details given in Table 4. The slit was always oriented at the parallactic angle (Filippenko 1982), and the long-slit spectra were reduced using standard procedures. Final spectra are shown in Figure 4. Some of the comparison spectra in Figure 4 were taken from the Berkeley SN spectral database⁴ as noted in the caption. The Lick/Kast spectra covered a wide wavelength range at low resolution in a blue and a red channel, while the MMT/BC spectra either covered a wide range in a single order (300 line mm^{-1} grating) or a smaller wavelength range with higher resolution (1200 line mm^{-1} grating) including Na I D $\lambda\lambda 5890$,

5896 and H α . For days 154 and 168 in Figure 4 we show a representative blackbody for comparison. All epochs exhibit strong line blanketing in the blue, and the characteristic temperature gets cooler with time as the transient fades rapidly. Narrow H α emission and the Ca II near-IR triplet in absorption remain prominent at all epochs.

In our moderate-resolution MMT spectrum taken on day 155 near the time of peak luminosity, we measure a total Na I D equivalent width (EW) of 4.3 ± 0.6 \AA . This is the total EW, including Galactic absorption and absorption in the local host galaxy (at the redshift of NGC 4490), as well as absorption in the photosphere of the transient; these components are blended at our observed resolution. Examining the spectra, the strong Na I absorption is blueshifted absorption that forms part of a P-Cygni profile with narrow Na I D emission. It is therefore likely that a large fraction of this absorption occurs in the wind/atmosphere of the transient source, and is therefore not a reliable measure of any local extinction. The Milky Way reddening value is $E(B - V) = 0.019$ mag, as noted above, but there may be additional local host-galaxy reddening. A value of $E(B - V) = 0.3$ mag for additional host reddening was inferred for the SN 2008ax by Pastorello et al. (2008), which is located nearby in the same galaxy, and below we discuss the likely value for the specific location of NGC4490-OT based on photometry of stars in the local environment. Any increase in the assumed reddening would increase our estimates of the peak luminosity of the transient, the inferred luminosity and mass of the progenitor, and the brightness of the dust-obscured source at visible wavelengths, but it would not change our estimate of the IR luminosity seen at late times.

2.5 Near-IR Spectroscopy

On 2014 June 7 we obtained a near-IR K -band spectrum at the position of NGC 4490-OT in its late-time aftermath of the outburst, using MOSFIRE on Keck. Although *Spitzer* data indicate a strong thermal-IR excess at this epoch, we did not detect continuum emission or any emission lines in our MOSFIRE spectrum with an exposure time of 1074 s.

3 DISCUSSION

3.1 Extinction and Environment

As is often the case, the nature of the progenitor star that one infers from a single-filter *HST* detection is clouded by the possibility of large and uncertain local extinction in the host galaxy. Local dust — especially circumstellar dust that surrounded the progenitor — may have been vaporised by the transient event, and there may be additional ISM extinction in this particular region of the host galaxy. To assist in our analysis of the progenitor below, we consider stars in the surrounding environment of NGC 4490-OT for additional constraints on the possible and likely local ISM extinction.

Figure 2 compares colours from the *HST* LE-GUS photometry, particularly in the UV and blue bands, to the colour-colour loci for normal supergiant stars, and also assumes a reddening vector following

⁴ <http://heracles.astro.berkeley.edu/sndb/>

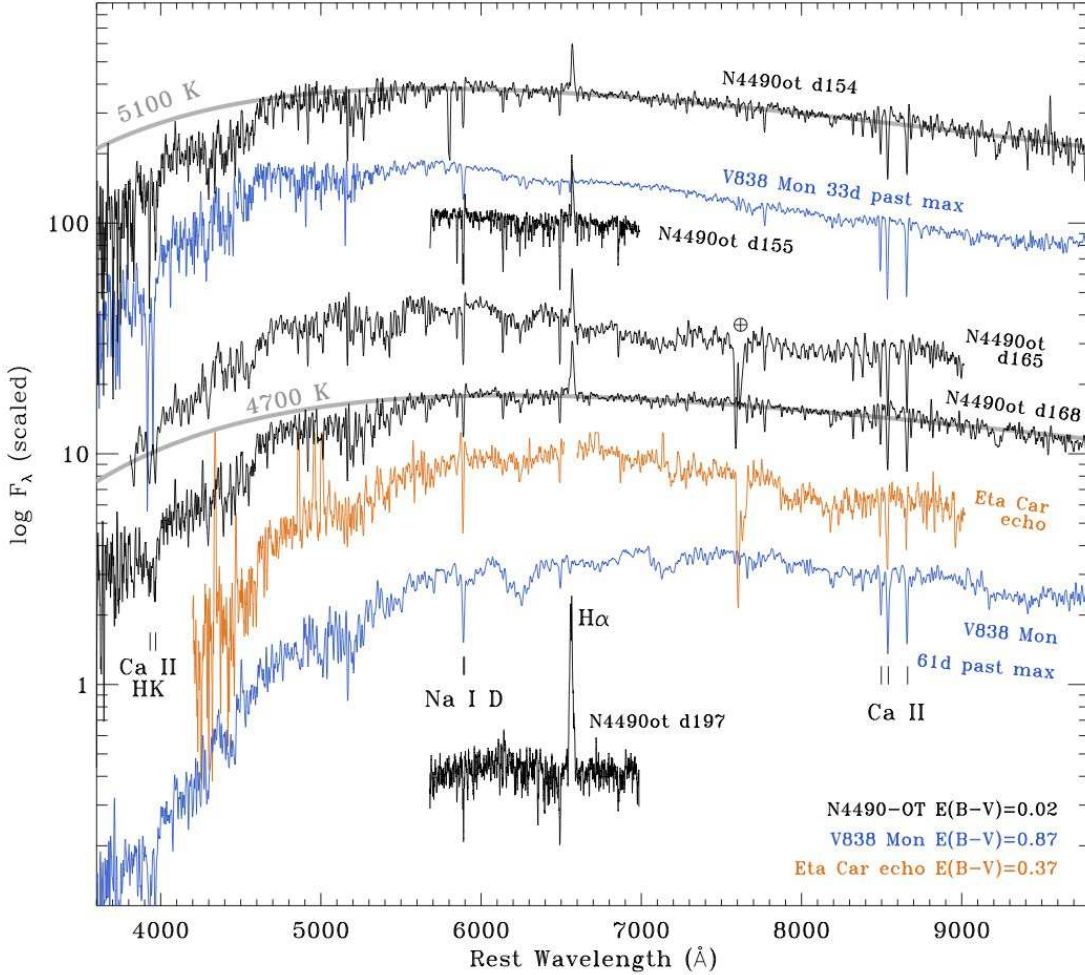


Figure 4. Optical spectra of N4490-OT compared to some spectra of V838 Mon. Details of our N4490-OT spectra are given in Table 4, and in this plot the spectra have been dereddened by a line-of-sight reddening value of $E(B - V) = 0.019$ mag. The spectra of V838 Mon were obtained with the Kast spectrograph at Lick Observatory on 2002 Mar. 11 and Apr. 8 (days 33 and 61, respectively, past the V -band peak of V838 Mon; see Munari et al. 2002). These V838 Mon spectra were taken from the Berkeley SN spectral database and have been discussed previously by Smith et al. (2011). The V838 Mon spectra are dereddened by $E(B - V) = 0.87$ mag (Munari et al. 2002, 2007). Although the days past maximum brightness of the V838 Mon spectra are not chronologically in step with the N4490-OT spectra, we chose to stagger them this way because N4490-OT had a much longer duration, and so these spectra represent comparable epochs during the decline from peak. We also include a spectrum of a light echo from η Carinae’s giant eruption (Rest et al. 2012), dereddened by $E(B - V) = 0.37$ mag as appropriate for our line of sight to the Carina Nebula (Smith, Barba, & Walborn 2004b).

Cardelli, Clayton, & Mathis (1989) with $R_V = 3.1$. In Figure 2, sources within a 100 pc projected radius of NGC 4490-OT are green open squares, and those projected within 50 pc are red open squares. For reference, the blue dashed line shows a reddening vector corresponding to $A_V = 3$ mag.

The resulting plot shows a great deal of scatter, indicating patchy and sometimes large extinction in the surroundings. Some stars in the surrounding 100 pc (green and red) have colours consistent with little or no reddening, while some show colours that suggest as much as 2 mag of V -band extinction. Indeed, it is apparent from the colour image in Figure 1 that NGC 4490 is speckled with patchy extinction. This holds true when we restrict ourselves only to the few sources within 50 pc (red). In the left panel of Figure 2 (F336W–F438W vs. F438W–F555W), one of the two red points at the top right of the plot corresponds to a star only a few (6–8) pixels from NGC 4490-OT, and this star has

a colour consistent with $A_V \approx 2$ mag. This might suggest rather large extinction in the immediate environment of the transient. On the other hand, many of the other stars have a range of values from $A_V \approx 0$ to $A_V \approx 2$ mag. Since choosing between these remains uncertain, in our analysis of the progenitor below we consider the impact of three different options for the adopted local reddening in addition to the Milky Way line-of-sight reddening. Option (1) corresponds to no additional local reddening as a lower limit, for option (2) we consider $A_V = 1.0$ mag as a likely value, and for option (3) we consider $A_V = 2.0$ mag as a likely upper limit to the local reddening.

3.2 Progenitor and Aftermath

The late-time *HST* images show a source at the same position as the progenitor, but fainter. This fading confirms the

candidate progenitor source first identified by Fraser et al. (2011).⁵

3.2.1 Progenitor

We measure an F606W absolute magnitude of -6.4 ± 0.24 for the progenitor around 6100 days before the transient was discovered (corrected only for Milky Way reddening). The pre-eruption *HST* data include only a single filter and only one epoch, but this offers some useful constraints on the possible nature of the progenitor. With no attempt at a bolometric correction, the progenitor system must be at least as luminous as the progenitor of SN 2008S (and almost as luminous as the progenitor of NGC 300-OT). Unlike SN 2008S and NGC 300-OT, however, this detection is at visible wavelengths, so the progenitor is not as heavily obscured by its own circumstellar dust.

On the other hand, the progenitor could also be blue, like the progenitor of SN 1954J and other LBVs. In this case the F606W absolute magnitude of -6.4 mag is a lower limit to the bolometric luminosity, because a bolometric correction or extinction correction must raise the progenitor's bolometric luminosity.

In fact, we favour the interpretation that the progenitor was a more luminous blue star, based largely on the IR non-detection of the progenitor in *Spitzer* data. The IR non-detections actually place strong constraints, provided that the star did not change substantially between 1994 (*HST* F606W image) and 2004 (*Spitzer* Bands 1 and 2). Of course, the star might have changed its luminosity and colour somewhat in this time if it was out of equilibrium and approaching a merger or some other disruptive event, so we can only take this information as approximate (moreover, if V1309 Sco or LBV eruptions like η Car provide guidance, the star may have been brightening and getting cooler as it approached its transient event, which would reinforce the analysis below). With this potential caveat aside, the *Spitzer* non-detections of the progenitor are quite constraining.

Figure 5 shows the SED of the candidate progenitor of NGC 4490-OT, as well as its aftermath (described below). We plot the *HST* F606W detection in 1994, plus the upper limits to λF_λ from our *Spitzer* IRAC Band 1 and 2 non-detections in 2004 (open blue diamonds). For the *HST* F606W detection of the progenitor we must assign an extinction correction, but this is uncertain, as noted above. Following an analysis of stars in the local environment of the transient, we consider three options for the extinction correction, and we plot all three of these on the SED in Figure 5. They are discussed below, along with implications for the nature of the progenitor.

Option 1: Here we correct only for the adopted line-of-sight Milky Way reddening of $E(B - V) = 0.02$ mag with zero additional reddening in the host galaxy. This is regarded as a lower limit. A blackbody through the F606W point and below the IRAC limits would need to have a temperature

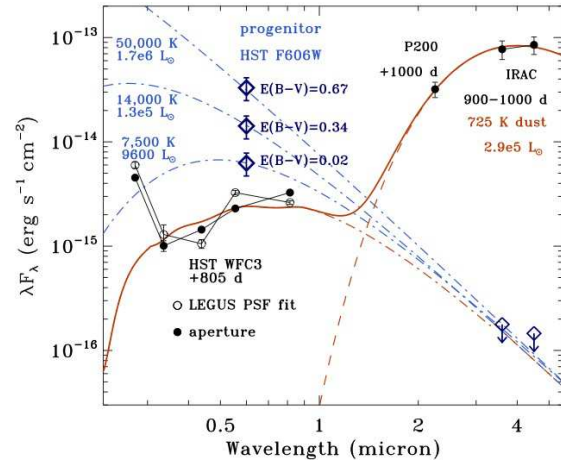


Figure 5. Observed SED of the progenitor of NGC 4490-OT (blue diamond symbols, including different reddening corrections; see text), as well as the source at the same position at late times (black circles and orange models). For the *HST* measurements of the late-time source, we show the results of PSF fitting photometry from the LEGUS photometric catalog (unfilled black circles) as well as aperture photometry using a $0''.5$ -diameter aperture (filled circles).

of at least 7500 K and a luminosity of more than $9600 L_\odot$. This would correspond to a relatively low-luminosity F-type supergiant or giant from an intermediate-mass star. This luminosity is more than an order of magnitude lower than the post-outburst IR luminosity.

Option 2: Next we consider adding $A_V = 1.0$ mag of local extinction ($E(B - V) = 0.32$ mag), so the total reddening is $E(B - V) = 0.34$ mag. We regard this reddening correction as a likely value, and it is similar to the value adopted for SN 2008ax by Pastorello et al. (2008). This F606W point and the IRAC limits would correspond to a blackbody with a temperature of at least 14,000 K (late B-type) and a luminosity of $1.28 \times 10^5 L_\odot$ or more. Such a star might be very similar to the class of lower-luminosity LBVs in their quiescent state, like HR Carinae or HD 168625 (Smith, Vink, & de Koter 2004a; Smith et al. 2011). They have effective initial masses (compared to single-star models) of $\sim 30 M_\odot$. For LBVs, there are of course significant caveats to an “initial mass” derived from single-star evolution models in cases where binary mass transfer or mergers may be relevant (see Smith & Tombleson 2015). Since the reddening is very uncertain, the temperature and luminosity could easily be somewhat more or less, but more reddening would simultaneously require the star to be more luminous and hotter, moving it roughly along the S Dor instability strip. This makes it seem plausible that the progenitor star was indeed a quiescent LBV. Interestingly, the luminosity of such a progenitor is within a factor of 2–3 of the post-outburst IR source’s luminosity, which would be consistent with the star surviving the event or with a merger product that is even more luminous than the progenitor. Interpreting the progenitor as a lower-luminosity LBV would also seem to be consistent with the relatively sparse environment in the vicinity of NGC 4490-OT (i.e., not in a massive cluster or H II region), since these lower-luminosity LBVs tend

⁵ Of course, some of the light contributing to this source could also be from a companion star, which may have been engulfed by the expanding dusty ejecta as in the case of V838 Mon, but in any case it is likely to represent the integrated flux of the system that gave rise to the transient source.

to be tens to hundreds of pc from clusters of O-type stars (Smith & Tombleson 2015).

Option 3: Next we consider adding $A_V = 2.0$ mag of local extinction ($E(B - V) = 0.65$ mag), based on the extinction inferred for the detected star nearest to the transient source, so the total reddening is $E(B - V) = 0.67$ mag. We regard this as a probable upper limit for the local ISM reddening within the host galaxy, although there may also have been considerable circumstellar extinction that was destroyed by the transient event. A blackbody through this F606W point and below the IRAC limits would need to be a very hot and luminous star, with $T \gtrsim 50,000$ K and $L \gtrsim 1.7 \times 10^6 L_\odot$. Such a star would be a very luminous early O-type main-sequence star or a WNH star with an initial mass around 80–100 M_\odot . Given the relative isolation of NGC 4490-OT in its host galaxy, this seems less likely than Option 2.

In any of the three options above, the IR upper limits do not allow the source detected by *HST* to be a cool evolved star like an asymptotic giant branch star or red supergiant. We therefore consider it quite plausible that the progenitor was a traditional LBV or related class of evolved luminous blue star (Option 2). Options 1 and 3 seem much less likely for the reasons noted above. In any case, it is interesting that the progenitor of N4490-OT is substantially more luminous and more massive than the expected progenitor systems of V838 Mon (roughly -1.5 mag; B-type star) or the low-mass progenitor of V1309 Sco (roughly $+4.8$ mag).

3.2.2 Aftermath

The position of the transient was observed again at late times with *HST*/WFC3, 805 days after discovery, and this time we have more colour information from multiple *HST* filter detections from the UV to near-IR. We also have a ground-based near-IR detection in the *K* band, plus clear detections with IRAC Bands 1 and 2 at four epochs between 300 and 1000 days after discovery. These late-time measurements of the SED are also plotted in Figure 5, where we choose the IRAC Band 1 and 2 photometry closest in time to the *HST* photometry; we do not see evidence of strong IR variability at 900–1000 days, only a gradual fading. For the late-time *HST* photometry, we show two measurements of the same data. The unfilled circles correspond to PSF-fitting photometry from the LEGUS photometric catalog (see Table 1, while the filled circles represent magnitudes measured using a $0''.5$ -diameter aperture.

In Figure 5, the observed photometry of the late-time source (black filled circles) is compared to a simple two-component model with a reddened hot star and warm dust. The reddened star is the same 14,000 K blackbody matched to the progenitor in Option 2 above, but reddened by $E(B - V) = 0.7$ mag.⁶ The dust component is a single-temperature 725 K grey body (λ^{-1} emissivity) that fits the *K*-band and IRAC points reasonably well. Given that this two-component model is probably quite oversimplified, the resulting combined model gives a fair representation of

⁶ Of course, one would not necessarily expect the post-outburst star to have the same temperature as the progenitor, so this is merely illustrative.

the observed photometry excluding the F275W point. The F275W measurement is admittedly somewhat strange; the F275W–F336W colour is steeper than the Rayleigh-Jeans tail of an unreddened blackbody, so it seems likely that the F275W filter has some strong contamination from Mg II $\lambda 2800$ line emission. Except for this point, it appears plausible that the post-outburst source is a luminous hot star enshrouded by its own circumstellar dust that was formed in the eruption event. In this sense, it conforms to traditional expectations for a giant LBV eruption.

3.2.3 Late-time IR (non)variability

The fact that the IRAC Band 1 and 2 fluxes have not dropped more substantially at late times is physically significant. A strong IR excess at late times indicates either pre-existing circumstellar medium (CSM) dust or dust that was newly formed in material ejected during the outburst. In any case, the dust could be heated by a luminous post-outburst source (indicating that the star likely survived the event), or it could be an “IR echo” wherein surrounding dust is heated by the pulse of UV/optical radiation from the transient event itself, and then re-emits its absorbed UV/optical energy in the thermal IR.

For an IR echo, the maximum dust temperature and the dust luminosity should fall with time as the light echo expands (see, e.g., Fox et al. 2011, 2015). The hottest dust will be found at the point of the light-echo paraboloid that is closest to the source, which is on the far side of the transient source in a spherical dust shell. This is at a radius of $r = ct/2$, where c is the speed of light and t is the time since the UV/optical peak of the transient source. For a pulse with peak luminosity L , the grain temperature of the hottest echo-heated dust at r is then given by

$$T_d^4 = \left(\frac{Q_{UV}}{Q_{IR}} \right) \frac{L}{16\pi r^2 \sigma},$$

where Q_{UV}/Q_{IR} describes the grain efficiency in the UV (absorption) and IR (emission), and σ is the Stefan-Boltzmann constant. At $t \approx 900$ –1000 d after the peak, when our *K*-band and second epoch of IRAC data were obtained, the minimum radius of the echo was $r \approx 0.8$ pc. At that radius the observed dust temperature of ~ 725 K would require a transient peak luminosity of roughly $1.1 \times 10^{12} L_\odot \times (Q_{UV}/Q_{IR})$. We don't know the grain properties *a priori*, but assuming a typical value of $Q_{UV}/Q_{IR} \approx 0.3$ would require an absolute magnitude of -23.6 mag. This is more luminous than any known SN, and of course vastly more luminous than the observed IR source, so we conclude that the observed colour temperature of the IR excess at late times is too hot to be explained by an IR echo. The dust must be located much closer to a central engine. Moreover, the temperature of the hottest echo-heated dust will fall as $T \propto t^{-0.5}$. At the time of our first epoch of IRAC observations around day 360, the maximum dust temperature should have been around 1200 K. This would shift the peak of the SED from $4 \mu\text{m}$ at day 1000 to around $2.4 \mu\text{m}$ at the earlier epoch. However, there is little change in the colour and IR luminosity between our IRAC epochs, adding further doubt to the IR-echo hypothesis.

On the other hand, the roughly constant post-outburst

IR luminosity is close to the reddening-corrected progenitor star's luminosity for our favoured Option 2 above. The factor of ~ 2 luminosity difference between the progenitor model of a 14,000 K star and the late-time IR luminosity could easily be accounted for by (1) a slightly higher temperature and luminosity for the progenitor for the same reddening (the IRAC upper limits only provide a lower limit to the star's temperature) or a somewhat higher reddening, (2) some contribution from an IR echo or residual luminosity from the fading eruption, or (3) an actual increase in the luminosity of the post-outburst source as one might expect if it were a stellar merger or if there was some other energy injection into the star's envelope. The pre- and post-outburst luminosities are, however, of the same order of magnitude, making it plausible that the relatively constant late-time IR excess is caused by a dust shell heated by a central surviving star.

For the IR luminosity of the dust shell, $L = 2.9 \times 10^5 L_{\odot}$, an equilibrium grain temperature of 725 K in a spherical shell corresponds to a radius of roughly 80 AU. To reach this radius by a time of ~ 900 d after ejection would require an expansion speed of roughly 160 km s^{-1} . Of course, small grains may be hotter than the equilibrium blackbody temperature, so the implied radius and required ejection speed may be a factor of 2-3 higher. As noted below, we infer ejection speeds from spectra of a few hundred km s^{-1} . Given factors of 2 or more owing to geometric uncertainty (we see evidence for asymmetry, as noted below), the observed IR SED at late times is reasonably consistent with expectations for emitting warm dust that formed from mass ejected in the 2011–2012 transient event. It is less likely that this is pre-existing dust, since dust at this same radius (~ 80 AU) would have been heated to a temperature of around 2200 K by the peak luminosity of the transient, and would therefore have been largely destroyed.

For standard assumptions about the grain density, an IR luminosity of $2.9 \times 10^5 L_{\odot}$ for 725 K dust requires an emitting mass of, very roughly, $10^{-9} M_{\odot}$ (see, e.g., Smith et al. 2003). The uncertainty may be a factor of 2 or more depending on assumptions about the grains, but then again, this is merely a lower limit to the dust mass since there may be a much larger mass of cool dust present and emitting primarily at far-IR wavelengths and unconstrained by our 3–5 μm data. The near-IR excess therefore gives little useful information about the total mass ejected in the event.

3.3 Visible-Wavelength Light Curve

From initial unfiltered magnitude estimates reported by amateur astronomers, NGC 4490-OT showed an initial peak at an absolute magnitude of roughly -13.5 , followed by a fast decline in the weeks after discovery (Figure 3). It then became unobservable because it was too close to the Sun during days 30–120 after discovery. When we began our unfiltered KAIT photometric monitoring after the source became observable again, we found it to be brighter than at discovery, and was rising again to a second peak at ~ 150 – 160 d, reaching an absolute unfiltered (approximately R -band) peak of -14.2 mag (correcting only for Milky Way extinction).

The source then faded rapidly for ~ 60 d after this second peak. Subsequently, the decline slowed, and the average

(interpolated) decline rate between days 220 and 800 was similar to the ^{56}Co decay rate (Figure 3), although we do not have data to characterize the details of the decline in this time interval. Unfortunately, we did not obtain multi-filter photometry to document the optical colour evolution during and after peak. However, our visible-wavelength spectra (see below) do show increasingly red colours and an evolution to cooler apparent temperatures during this time, as the source faded from peak. In fact, the colours became quite red at the latest epochs observed by *HST* at day 805, with a strong IR excess.

The light curve of NGC 4490-OT, with multiple peaks and an evolution to red colours and IR excess, is qualitatively reminiscent of the complex multi-peaked light curves observed in some Galactic transients that have been described as stellar merger events. Both V838 Mon and V1309 Sco show an initial blue peak with a rapid decline on a time scale similar to that of NGC 4490-OT, and a comparably luminous second or third peak after that with increasingly red colour. The light curves of these two objects are shown in Figure 3. An important difference in the light curves, however, is that NGC 4490-OT had a much higher peak luminosity, and a longer duration. V1309 Sco faded in about one month and V838 Mon faded in 80–90 days, while NGC 4490-OT stayed bright for ~ 200 days. Interestingly, the duration and brightness of these events appears to correlate with the suspected mass of their progenitor stars, as we discuss later. The 19th century Great Eruption of η Carinae also showed multiple narrow peaks followed by a longer broad plateau (Smith & Frew 2011), and its duration was a decade or more. Since η Car is likely to be a much more massive star, it may extend this same correlation.

The bright phase of the transient (days 0–200) is poorly sampled because the source's position in the sky was near the Sun for much of this time. Simply interpolating between observation dates and integrating the optical luminosity can give a crude estimate of the total radiated energy (ignoring any bolometric correction) of very roughly $E_{\text{rad}} \approx 1.5 \times 10^{48}$ ergs. This is less than η Car's giant eruption, but substantially more than other less-energetic LBV eruptions like P Cygni (Smith & Hartigan 2006; Smith et al. 2011) or SN 1954J (Humphreys, Davidson, & Smith 1999). It is also orders of magnitude more than the lower-mass stellar merger sources mentioned above.

3.4 Spectroscopic Evolution

Figure 4 shows the evolution of the visible-wavelength spectrum of NGC 4490-OT. Unfortunately, we were not able to obtain any early-time spectra. As noted above, however, Magill et al. (2011) reported that early-time spectra showed a blue continuum with bright narrow Balmer emission lines reminiscent of LBVs. Our spectra document times just before the second peak, which is the time of maximum observed luminosity, and the rapid decline from this main peak. At these phases, NGC 4490-OT showed a warm continuum consistent with temperatures around 5000 K, accompanied by weak $\text{H}\alpha$ emission, strong Ca II absorption (both the H&K lines and the near-IR triplet), and strong metal line-blanketing absorption in the blue.

This apparent temperature around 5000 K is similar to that indicated by spectroscopy of light echoes from η

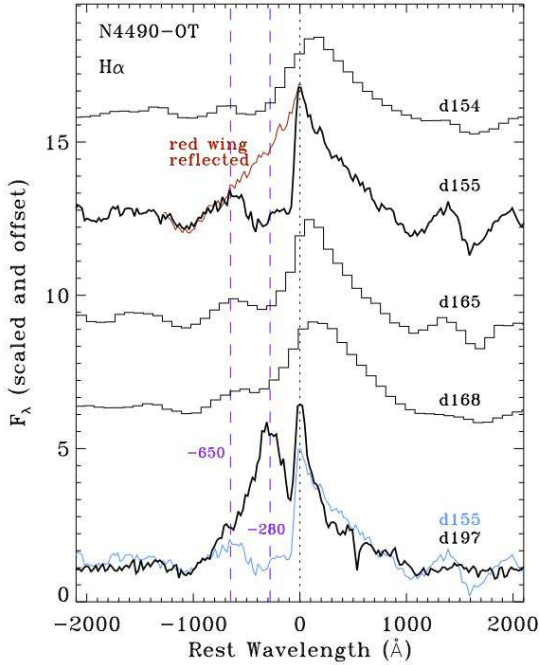


Figure 6. Details of the $H\alpha$ line profiles in our spectra of NGC 4490-OT. The two MMT spectra on days 155 and 197 have higher spectral resolution than the other three. The spectrum in red plotted over the day 155 spectrum shows what the $H\alpha$ line profile would look like if it were symmetric, by taking the red wing of the line and reflecting it to the blue side of the line. Also, the day 155 spectrum is reproduced in blue and plotted over the last epoch on day 197 for comparison, showing that the blueshifted absorption on day 155 occurred at similar velocities to the excess blue emission on day 197. Representative velocities of -650 km s^{-1} (blue edge of the absorption) and -280 km s^{-1} (middle of the absorption trough and emission peak) are shown with purple dashed lines.

Carinae’s 19th century eruption (Rest et al. 2012). Similar absorption features were also seen in the light echo spectra of η Car and some extragalactic LBVs like UGC 2773-OT (Rest et al. 2012; Smith et al. 2011, 2016).

Interestingly, the spectra of NGC 4490-OT do not show the forbidden $[\text{Ca II}] \lambda\lambda 7291, 7323$ doublet in emission (or the Ca II near-IR triplet in emission), which is another way that NGC 4490-OT seems distinct from SN 2008S-like objects (Prieto et al. 2008; Thompson et al. 2009; Bond et al. 2009; Berger et al. 2009; Smith et al. 2009). The spectra of NGC 4490-OT during its decline do, however, bear a striking resemblance to spectra of the Galactic transient V838 Mon during its decline from peak luminosity (Munari et al. 2002, 2007). Figure 4 compares our spectra of NGC 4490-OT to those of V838 Mon. (While the times after peak of 30–70 days for V838 Mon are different than for the day 150–200 spectra of NGC 4490-OT, these trace similar epochs during the decline because NGC 4490-OT had a much longer timescale, fading at 180–200 days instead of ~ 80 days for V838 Mon). Spectra of both objects show a similar evolution in apparent continuum slope, they both exhibit a similar forest of narrow atomic absorption lines and line blanketing in the blue that are characteristic of yellow F and G-type supergiants, and both have very strong Ca II absorption in the

$H\&K$ lines, as well as strong absorption in the Ca II near-IR triplet.

A notable difference is that V838 Mon did not exhibit strong $H\alpha$ in emission during these epochs, whereas NGC 4490-OT did. (V838 Mon did, however, show $H\alpha$ emission at some earlier epochs; Munari et al. 2007.) The emission EW rises from about -14 \AA at peak (we measure $-14.5 \pm 0.5 \text{ \AA}$ on day 155, with similar values and larger uncertainty in the lower-resolution spectra around the same time) to $-92.6 \pm 3 \text{ \AA}$ as it was fading quickly on day 197. $H\alpha$ seen in emission for a longer time may be indicative of a higher mass-loss rate in NGC 4490-OT than V838 Mon, and in this respect, NGC 4490-OT is more akin to LBVs with $H\alpha$ emission in eruption. Unfortunately, little work has been done using radiative-transfer models to derive quantitative physical parameters from the $H\alpha$ strength in a giant LBV eruption.

Even without such radiative-transfer models, however, the $H\alpha$ line profile can provide some interesting physical information about the kinematics of the NGC 4490-OT transient event. Figure 6 shows the $H\alpha$ line profile in our five epochs of spectroscopy for this object. In this plot, zero velocity is determined from the centroid of extended narrow (unresolved) $H\alpha$ emission along the slit, arising from H II regions in the same region of the host galaxy. Of these 5 epochs, the two MMT spectra with relatively high resolution ($1200 \text{ line mm}^{-1}$ grating; days 155 and 197) are the most informative.

The $H\alpha$ line near peak (day 155) shows an asymmetric P Cygni-like profile. (The spectra from days 154, 165, and 168 are consistent with a similar line profile observed with degraded resolution.) In Figure 6, we take the red side of the line and reflect it about zero velocity and plot it over the blueshifted side of the line; this reflected red wing is shown in red. At velocities of -650 to -1200 km s^{-1} , the reflected red wing overlaps well with the blue wing, but the blueshifted side of $H\alpha$ shows a pronounced deficit at 0 to -650 km s^{-1} . This comparison gives a strong indication that the underlying emission component of $H\alpha$ is a symmetric triangular profile, and that the asymmetry is caused by strong blueshifted self-absorption arising from a dense outflow with expansion speeds up to 650 km s^{-1} . The blue edge (-650 km s^{-1} , representing the maximum outflow speed along the line of sight) and the centroid of the P-Cygni absorption trough (roughly -280 km s^{-1} , perhaps representing the bulk outflow speed) are marked with dashed vertical purple lines in Figure 6. This outflow speed is reminiscent of the nebula around η Car (Smith 2006), which has expansion speeds ranging from about 40 km s^{-1} at the equator to 650 km s^{-1} at the pole. Note that the extremes of the line wings are probably broadened by electron scattering, and do not necessarily reflect the maximum expansion speed.

These representative speeds in the P-Cygni absorption profile at peak luminosity (day 155) become quite interesting when we examine the later spectrum on day 197, during the rapid decline after peak (Figure 6). It also shows an asymmetric profile, but this time it has excess blueshifted emission instead of absorption. Indeed, the $H\alpha$ line profile has a strong blueshifted emission bump with a similar centroid at -280 km s^{-1} and a comparable range of speeds as the absorption trough seen earlier on day 155. In Figure 6, we overplot the day 155 $H\alpha$ profile (in blue) on the day 197

spectrum for comparison, and the purple vertical dashed lines show speeds of -650 and -280 km s $^{-1}$ for reference.

The H α profile with the strong blue emission bump on day 197 is quite unusual, but some similar features have been seen before. A comparable blue emission bump in H α was recently reported in the late-time spectra of UGC 2773-OT, which is a decade-long LBV-like eruption similar to η Carinae (Smith et al. 2016). In the same analysis, Smith et al. (2016) also showed that line emission from the present-day bipolar nebula around η Car shows a similar blue emission bump. An asymmetric blue bump in H α has also been seen at faster speeds in several SNe IIn (Smith et al. 2012a,b, 2015; Fransson et al. 2014), usually attributed to bipolar or perhaps disk-like geometry in the shock interaction. A corresponding red bump is usually assumed to be weaker or absent owing to extinction by dust or occultation by the opaque SN ejecta. Radiative-transfer simulations of SNe IIn with bipolar CSM support these expectations of having an asymmetric blue emission line arising from a bipolar geometry (Dessart et al. 2015).

A plausible interpretation is that a massive shell was ejected at these speeds and was initially seen in absorption, but as the underlying photosphere cooled (as indicated by the spectral evolution during the decline from peak) and as the optical depth dropped, the same dense shell is seen in H α emission. This likely indicates ongoing shock heating of this ejected shell. The fact that the line is asymmetric at late times either requires that the mass ejection was intrinsically asymmetric with most of the mass ejected toward our observing direction, or that the receding side of the ejected shell is obscured by large amounts of dust that formed in the outflow. The large IR excess flux and fading of the optical source at late times are qualitatively consistent with copious dust formation in the ejecta.

3.5 Stellar Merger Events Across a Diverse Range of Initial Mass

In preceding sections, we noted a qualitative similarity between NGC4490-OT and Galactic transient events that have been interpreted as stellar mergers: V1309 Sco (Tylenda et al. 2011) and V838 Mon (Bond et al. 2003; Munari et al. 2002). The observed similarities apply to their somewhat irregular multi-peaked light curves, as well as to the morphology of their spectra. The comparison may extend to other proposed merger objects as well, such as V4332 Sgr in 1994 (Martini et al. 1999), OGLE 2002-BLG-360 (Tylenda et al. 2013), M85-2006-OT1 (Kulkarni et al. 2007), and M31 RV (Rich et al. 1989), although we did not discuss these in detail. CK Vul also had a multi-peaked light curve (Shara et al. 1985).

The progenitor of NGC 4490-OT detected in pre-eruption *HST* data was a more massive star than either V838 Mon or V1309 Sco. Based on our favoured value for the local reddening, we inferred that the progenitor could be quite similar to the lower-luminosity group of LBVs (Smith, Vink, & de Koter 2004a), with an effective initial mass of around $30 M_{\odot}$. As noted earlier, NGC 4490-OT appears in a relatively isolated region of its host galaxy, similar to the lower-luminosity LBVs (Smith & Tombleson 2015).

If indeed NGC 4490-OT was a merger event, then it would appear to extend a correlation seen in the lower-mass

mergers. Based on a statistical analysis of published candidate merger events, Kochanek et al. (2014) suggested that there is a correlation between the progenitor’s initial mass and the peak luminosity of the transient resulting from the putative merger. NGC 4490-OT seems to agree with this, since it had a more massive progenitor star than either V1309 Sco and V838 Mon, and also had a substantially higher peak luminosity. The initial mass is uncertain, but for $20\text{--}30 M_{\odot}$, this agrees reasonably well with the trend reported by Kochanek et al. (2014).

We note another possible correlation as well. In addition to a correlation between initial mass and transient peak luminosity, we note that there may be a correlation between both of these and the duration of the event. V838 Mon had a longer duration than V1309 Sco, and NGC 4490-OT had a significantly longer duration than V838 Mon. There is a simple physical motivation for both of these trends. A merger event from more massive stars has more kinetic energy and angular momentum at the time of the merger, perhaps providing more thermal energy in the merger and a brighter transient event. Similarly, more massive stars that merge must shed some fraction of their mass and angular momentum in the event. If more mass is ejected, the diffusion time is longer for the ejected envelope mass.

Interestingly, η Carinae would seem to extend these same trends, if it were considered as some sort of binary interaction event. It is a much more massive star, and the transient event was somewhat more luminous at peak and much longer lasting (a decade) than NGC 4490-OT. In fact, merger models have already been suggested as possible explanations for η Car’s 19th century eruption (Kenyon & Gallagher 1985; Gallagher 1989; Podsiadlowski 2010), although these have the obvious difficulty of explaining why η Car also had multiple major eruptions in the past. Grazing collisions at periastron have also been discussed as playing a role in the eruptions (Smith 2011). The emitting photosphere during η Car’s eruption was bigger than the current periastron separation, so some sort of violent interaction must have occurred (Smith 2011), although whether this was a driving mechanism, a trigger, or merely an after-effect remains uncertain. It is interesting that η Car shares many of the observational hallmarks of the other stellar merger events: irregular multi-peaked light curve (Smith & Frew 2011), transition to redder colours after peak (Prieto et al. 2014), followed by dust formation and post-outburst obscuration (Smith et al. 2003). We have shown in this paper that published light-echo spectra of η Car (Rest et al. 2012) also resemble our spectra of NGC 4490-OT and spectra of V838 Mon at some epochs.

The physical mechanism to power giant LBV eruptions is still not understood, but if stellar mergers or collisions are viable culprits, then it may be useful to consider them in context with low-mass stellar merger events as contributing to the pool of observed non-SN transient sources. LBVs may be the more massive extension of these other eruptive merger events, and that extension may be continuous. Massive LBV stars are more rare, but in terms of triggering merger events in close binary systems, LBVs have the physical advantage that they can change their radius suddenly when they inflate as part of their S Doradus variability. This change may instigate mass transfer or a merger in a binary system that was previously not interacting. Folding in se-

lection effects, their higher mass and energy budgets, with higher peak luminosities and longer durations, may compensate for their relative rarity, to allow LBV mergers to make a significant contribution to observed extragalactic SN impostor statistics. In any case, if some or all giant LBV eruptions are indeed produced by merger or collision events, then it becomes more difficult to confidently classify SN impostors as LBVs, SN2008S-like objects, or something else.

ACKNOWLEDGEMENTS

Some of the data reported here were obtained at the MMT Observatory, a joint facility of the University of Arizona and the Smithsonian Institution. We thank the staffs at Lick and MMT Observatories for their assistance with the observations. We also appreciate the help of Jeff Silverman for some of the Lick observations. Data from Steward Observatory facilities were obtained as part of the observing program AZTEC: Arizona Transient Exploration and Characterization. Lindsey Kabot assisted with early stages of the MMT spectral data reduction. The work presented here is based in part on observations made with the NASA/ESA *Hubble Space Telescope*, obtained at the Space Telescope Science Institute, which is operated by the Association of Universities for Research in Astronomy, Inc., under NASA contract NAS5-26555. These are based in part on observations associated with program #13364 (Legacy ExtraGalactic UV Survey, LEGUS). This paper has made use of the higher-level data products provided by the LEGUS team.

N.S. and J.E.A. received partial support from National Science Foundation (NSF) grants AST-1210599 and AST-1312221. M.M.K. acknowledges support from the Carnegie-Princeton fellowship. Funding for this effort was provided in part by the *Spitzer* SPIRITS Cycles 10–12 exploration science program. The supernova research of A.V.F.'s group at U.C. Berkeley presented here is supported by Gary & Cynthia Bengier, the Christopher R. Redlich Fund, the TABASGO Foundation, and NSF grant AST-1211916. KAIT and its ongoing operation were made possible by donations from Sun Microsystems, Inc., the Hewlett-Packard Company, AutoScope Corporation, Lick Observatory, the NSF, the University of California, the Sylvia & Jim Katzman Foundation, and the TABASGO Foundation. Research at Lick Observatory is partially supported by a generous gift from Google. J.J. is supported by an NSF Graduate Research Fellowship under Grant No. DGE-1144469.

REFERENCES

Adams, S.M., et al. 2015, preprint, arXiv.151107.7393
 Afşar, M., & Bond, H.E. 2007, *AJ*, 133, 387
 Berger E, et al. 2009, *ApJ*, 699, 1850
 Bond, H.E. 2011, *ApJ*, 737, 17
 Bond H.E., Bedin L. R., Bonanos A. Z., Humphreys R. M., Monard L. A. G. B., Prieto J. L., Walter F. M., 2009, *ApJ*, 695, L154
 Bond H.E., Henden A, Levay ZG, et al. 2003, *Nature*, 422, 405
 Bond, H.E., & Siegel, M. H. 2006, *AJ*, 131, 984
 Calzetti, D., Lee, J. C., Sabbi, E., et al. 2015, *AJ*, 149, 51
 Cardelli, J. A., Clayton, G. C., & Mathis, J. S. 1989, *ApJ*, 345, 245
 Cortini G., & Antonelli S. 2011, *CBET*, 2789, 1
 Dessart L., Audi E., Hillier D.J. 2015, *MNRAS*, 449, 4304
 Dolphin, A. E. 2000, *PASP*, 112, 1383
 Fazio G, et al. 2004, *ApJS*, 154, 10
 Filippenko A.V. 1982, *PASP*, 94, 715
 Filippenko, A. V., Li, W. D., Treffers, R. R., & Modjaz, M. 2001, in *Small-Telescope Astronomy on Global Scales*, ed. W. P. Chen, C. Lemme, & B. Paczyński (San Francisco: ASP), 121
 Filippenko A. V. 2003, in *From Twilight to Highlight: The Physics of Supernovae*, ed. W. Hillebrandt & B. Leibundgut (Berlin: Springer), 171
 Fox O.D., et al. 2011, *ApJ*, 741, 7
 Fox O.D., et al. 2015, in press
 Fransson C., et al. 2014, *ApJ*, 797, 118
 Fraser, M., Kotak R., Magill L., et al. 2011, *ATel*, 3574, 1
 Gallagher J. S., 1989, in *Davidson K., Moffat A. F. J., Lamers H. J. G. L. M., eds, Physics of Luminous Blue Variables*. Kluwer, Dordrecht, p. 185
 Gogarten, S. M., Dalcanton, J. J., Murphy, J. W., et al. 2009, *ApJ*, 703, 300
 Humphreys R. M., Davidson K., 1994, *PASP*, 106, 1025
 Humphreys R.M., Davidson K, Smith N. 1994, *PASP*, 111, 1124
 Ivanova N, Justham S, Avendano Nandez JL, Lombardi JC. 2013, *Science*, 339, 433
 Kaminski M., Menten K.M., et al. 2015, *Nature*, 520, 322
 Kato T. 2003, *A&A*, 399, 695

Kenyon S. J., Gallagher J. S., 1985, *ApJ*, 290, 542
 Kochanek C.S. 2011, *ApJ*, 741, 37
 Kochanek C.S., Adams S.M., Belczynski K. 2014, *MNRAS*, 443, 1319
 Kulkarni S.R., et al. 2007, *Nature*, 447, 458
 Kurtenkov A., et al. 2015, *A&A*, in press (arXiv:1505.07808)
 Li, W., Filippenko, A. V., Van Dyk, S. D., Hu, J., Qiu, Y., Modjaz, M., & Leonard, D. C. 2002, *PASP*, 114, 403
 Loebman S.R., et al. 2015, *AJ*, 149, 17
 Magill L., Kotak R., Fraser M., Smartt S. 2011, *CBET*, 2789, 1
 Martini P., Wagner R.M., Tomaney A., Rich R.M., Della Valle M., Hauschildt P.H. 1999, *AJ*, 118, 1034
 Mason E, Diaz M, Williams RE, Preston G, Bensby T. 2010, *A&A*, 516, A108
 Mayall M.W. 1949, *AJ*, 54, 191
 Miller J.S., Stone R.P.S. 1993, *Lick Obs. Tech. Rep. 66* (Santa Cruz: Lick Obs.)
 Munari U, Henden A, Kiyota S, et al. 2002, *A&A*, 389, L51
 Munari U, Navasardyan H, Villanova S. 2007, in *The Nature of V838 Mon and it Light Echo*, ASP Conf. Ser. 363, ed. R.L.M. Corradi & U. Munari (San Francisco: ASP), 13
 Nichols C.P., et al. 2013, *MNRAS*, 431, L33
 Pastorello A., Kasliwal, M., Crockett, R.M., et al. 2008, *MNRAS*, 389, 955
 Podsiadlowski P., 2010, *New Astron. Rev.*, 54, 39
 Prieto J. L., 2008, *The Astronomers Telegram*, 1550, 1
 Prieto JL, Kistler MD, Thompson TA, et al., 2008, *ApJ*, 681, L9
 Prieto JL, et al. 2014, *ApJ*, 787, 8
 Rest A. et al., 2012, *Nature*, 482, 375
 Rich RM, Mould J, Picard A, Frogel JA, Davies R. 1989, *ApJ*, 341, L51
 Rosero-Rueda VA, Bond HE, Exter KM, Schaefer GH, Plata A. 2008, *RevMexAA*, 34, 135
 Schlafly E.F., & Finkbeiner D. 2011, *ApJ*, 737, 103
 Shara, M. M., Moffat, A. F. J., & Webbink, R. F. 1985, *ApJ*, 294, 271
 Smith N. 2006, *ApJ*, 644, 1151
 Smith N. 2011, *MNRAS*, 415, 2020
 Smith N. 2014, *ARA&A*, 52, 487
 Smith N., Barba, R.H., & Walborn, N.R. 2004b, *MNRAS*, 351, 1457
 Smith N., Cenko S.B., Butler N., et al. 2012b, *MNRAS*, 420, 1135
 Smith N., & Frew D. J. 2011, *MNRAS*, 415, 2009
 Smith N., Ganeshalingam M., Chornock N.R. et al. 2009, *ApJ*, 697, L49
 Smith N., & Hartigan, P. 2006, *ApJ*, 638, 1045
 Smith N., Humphreys RM, Gehrz RD. 2001, *PASP*, 113, 692
 Smith N., Gehrz R. D., Hinz P. M., et al. 2003, *AJ*, 125, 1458
 Smith N., Miller A., Li W., et al. 2010a, *AJ*, 139, 1451
 Smith N, & Owocki SP 2006, *ApJ*, 645, L45
 Smith N, & Tombleson R. 2015, *MNRAS*, 447, 603
 Smith N., Vink J., de Koter A., 2004a, *ApJ*, 615, 475
 Smith N., et al. 2011, *MNRAS*, 415, 773
 Smith N., et al. 2012a, *AJ*, 143, 17
 Smith N., et al. 2015, *MNRAS*, 449, 1876
 Smith N., et al. 2016, *MNRAS*, 455, 3546
 Soker N, & Tylenda R. 2006, *MNRAS*, 373, 733
 Soker N, & Tylenda R. 2007, in *The Nature of V838 Mon and it Light Echo*, ASP Conf. Ser. 363, ed. R.L.M. Corradi & U. Munari (San Francisco: ASP), 280
 Sparks W. B. et al., 2008, *AJ*, 135, 605
 Tammann G. A., Sandage A., 1968, *ApJ*, 151, 825
 Thompson T. A., Prieto J. L., Stanek K. Z., Kistler M. D., Beacom J. F., Kochanek C. S., 2009, *ApJ*, 705, 1364
 Tylenda R, Hajduk M, Kaminski T, et al. 2011, *A&A*, 528, A114
 Tylenda R, et al. 2011, *A&A*, 555, A16
 Van Dyk S. D., Filippenko A. V., Chornock R., Li W., Challis P. M. 2005, *PASP*, 117, 553
 Van Dyk S. D., Peng C. Y., King J. Y., et al. 2000, *PASP*, 112, 1532
 Williams SC, Darnley MJ, Bode MF, Steele IA. 2015, in press (arXiv:1504.07747)